Repairing stress induced cracks in the Keck primary mirror segments

Dennis McBride, John S. Hudek, Sergey Panteleev

W.M. Keck Observatory, 65-1120 Mamalahoa Hwy., Kamuela HI, USA 96743

ABSTRACT

Stress induced cracks have developed in the Zerodur glass at bonded supports for the primary mirror segments of the W.M. Keck Observatory telescopes. This has been a slow process that has advanced over the 20 year life of the telescopes. All mirror segments exhibit cracks to varying degrees. The number and severity of cracks has now reached a stage at which repairs are mandatory. A project is under way to determine the root causes of the cracks, and to develop a repair strategy. New supports and bonding methods are being designed and tested that will replace all of the original supports.

Keywords: Keck, mirror segment, stress, crack, axial insert, radial pad, Zerodur

1. INTRODUCTION

The W.M. Keck Observatory (WMKO) operates two optical / infrared telescopes at an elevation of 4145 meters on Mauna Kea on the island of Hawaii. The primary mirrors are 10 meters in diameter, made up of 36 hexagonal segments which are 1.8 meters vertex to opposite vertex, and approximately 75 mm thick. The mirrors are Zerodur low expansion glass ceramic by Schott AG, having coefficient of thermal expansion (CTE) of 0 ± 10^{-7} ºC^{-1} as measured at production [1]. The nighttime temperature on Mauna Kea is normally 0 ± 8ºC, and the telescope domes are refrigerated during the daytime.

The telescopes are a Richey-Chrétien design. The primary mirror surface is hyperbolic with a 34.974 meter radius of curvature and a conic constant of -1.003683[2]. There are six different segment types which are formed as off-axis hyperbolic sections to make up the primary mirror, as shown in Figure 1. There are two spare segments of each type, which are rotated into the telescopes during segment re-coatings.

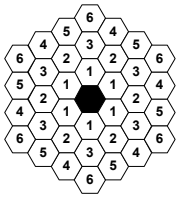

Figure 1. Keck primary mirror segment types.

The back of a segment is polished spherically convex with 35 meter radius in order to maintain an approximately constant thickness across the glass surface. Each primary mirror segment is supported by two kinematically decoupled support systems for the radial (in plane) and axial (normal) loads.

For the radial support, a central hole is machined into the center of the back surface. The hole is 254mm diameter, and 55mm deep. Six equally spaced support pads of Invar 36 material are bonded to the circumference of the hole, with the center line of the pads at the mid-plane of the segment. The adhesive used is Hysol EA-9313 epoxy with bond line thickness of approximately 0.76mm. The six radial pads are connected by flexures to a support ring and the radial support post. A diaphragm in the radial post provides isolation between the radial and axial supports.

Axial support is provided by 36 axial inserts of Invar 36 material, which are bonded at the bottom of 18mm diameter by 39mm deep holes in the back of the segment. The adhesive is Hysol EA-9313 with 0.25mm bond line. The bond line is positioned at the mid-plane of the segment in order to minimize front surface deflections due to bending moments that are applied by the bonded inserts. Subsequent analysis has shown that this is less of a concern than originally expected. The axial supports for newer segmented mirror designs are bonded on the back surface of the segments.

Ground-based and Airborne Telescopes IV, edited by Larry M. Stepp, Roberto Gilmozzi, Helen J. Hall,
Proc. of SPIE Vol. 8444, 844421 · © 2012 SPIE · CCC code: 0277-786/12/$18 · doi: 10.1117/12.926566

The axial inserts are connected by flexible rods to three whiffletree structures which distribute the axial load. A system of adjustable warping beams is attached to the whiffletree structures to allow fine correction of the front surface figure. The axial inserts carry a maximum axial force of ± 310 N for gravity and warping loads. The total weight of a mirror segment and whiffletree assemblies is 4493 N.

The radial post and whiffletrees ultimately are connected to a sub-cell assembly. A diagram of a mirror segment is shown in Figure 2, and a cross-section through the radial post in Figure 3.

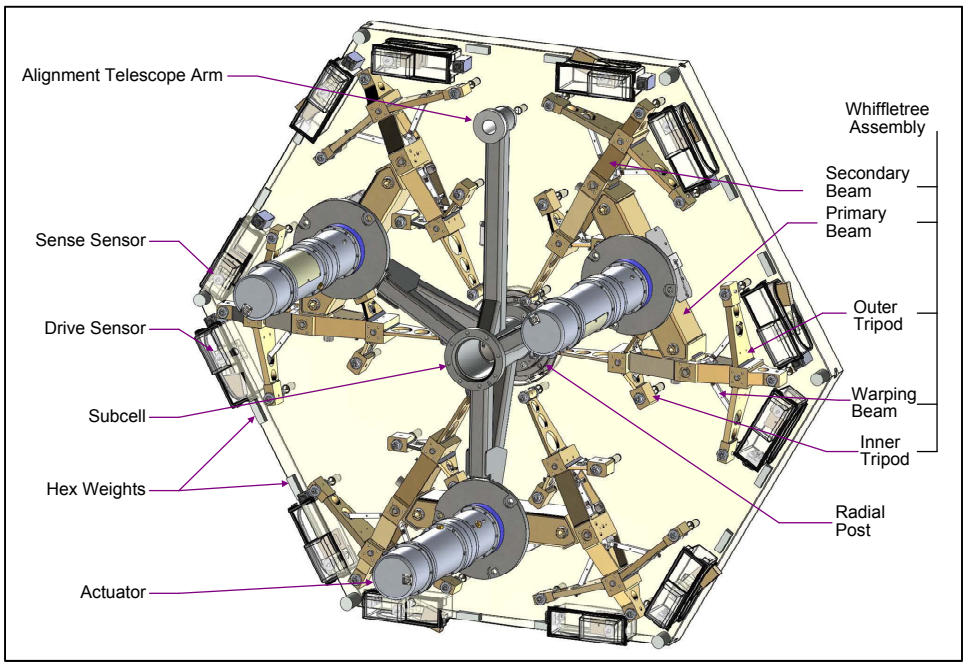

Figure 2. Keck primary mirror segment.

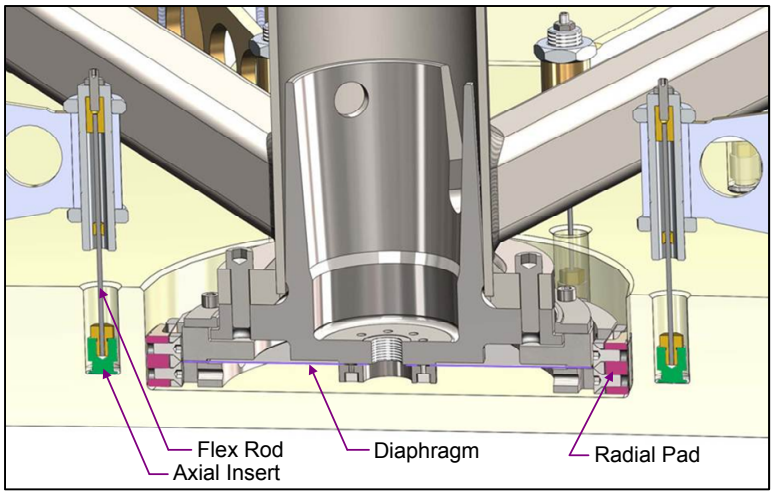

Figure 3. Mirror segment cross section at radial post.

In addition to the 36 axial inserts which support the axial segment load, there are 12 axial inserts which support the position sensors near the segment vertices. These adjust the phasing of each segment relative to its neighbors. (Dummy weights are installed in positions where there are no neighbors.) One additional insert is used as a reference for clocking the segment in the mirror cell. Overall, there are 49 axial inserts in each mirror segment.

2. PROJECT HISTORY

Mirror segments were fabricated between 1988 and 1992. Blanks for the mirror segments were manufactured by Schott AG. Polishing was performed by Itek and Tinsley. Machining and assembly were performed by Itek. Ion figuring was performed by Kodak.

The initial specifications for the segment optics indicated that there should be no "hairline or conchoidal fractures on any surface."[3] It is believed that the segments were originally manufactured with sufficient care that there were no visible cracks. From 1994 to 2007, cracks were found and repaired in radial pads of nine segments. The first of these was caused by a handling error when a segment was being removed from the telescope for re-coating. This repair was performed by a team from Itek. Subsequent repairs were performed in house by WMKO staff. However, the specific cause of the cracks and justification for their repair is not documented.

To repair the radial pad cracks the radial post and pad were removed. The damaged glass surface was ground out to a larger radius with a custom fixture, then etched. A new radial pad with a matching radius was machined and bonded in place. A photo of the radial pad support ring is in Figure 4, a radial pad in Figure 5, and a repaired pad in Figure 6.

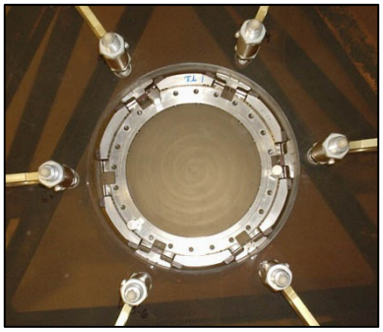

Figure 4

Figure 5

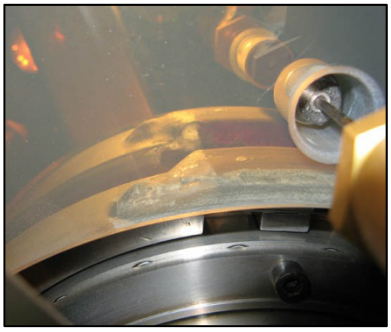

Figure 6

An investigation of the mirror crack problem started in 2008 by a team of WMKO personnel. The extent and severity of cracks led to the initiation of the Mirror Repair Project in December 2008. The initial focus was on the radial pads, since there was a history of repairs, and they had the most obvious damage. Because the cause of the cracks was unknown and it was felt that handling the segments could result in further damage, the segment exchange and re-coating process was put on hold while the problem was investigated.

A finite element analysis (FEA) program was started in March 2009 to understand the stresses the at radial pad bonds. This analysis was performed by Ozen Engineering in Sunnyvale, California. Analysis results are discussed in Section 6.

In August 2009 a review of the segment handling procedures was conducted. Steps in the procedures where accidental mishandling could result in overturning loads and large stresses placed on the radial pads were identified. Engineering and procedural changes were put in place to reduce these risks.

A photographic survey of the mirror segments was started in August 2009. Evaluation of the photos from the first few segments surveyed indicated that there were numerous cracks in the axial inserts as well. These are small and difficult to see by eye. They can only be viewed through the front surface of the mirror when the aluminum coating has been removed. It was noted that there was one segment on which an axial insert had completely failed. In this condition the whiffletree cannot properly distribute the load among the axial inserts, and it is not possible to apply warping loads to the segment. It was at this point that the focus shifted to the axial inserts. As the photo survey progressed, it became obvious that there were extensive cracks at the axial insert bonds.

Radial pad cracks, although still being monitored carefully, are fairly stable at this time. The improvement in handling procedures has reduced the chance of a major radial pad failure.

Since 2009, a new axial insert has been designed. Numerous tests have been performed to evaluate the performance of the new insert, adhesives, and the effects of surface finish and etching on the surface strength Zerodur. An external review of the new insert design was held in October 2011. The design was approved, with recommendations for additional testing. Construction of a repair facility at the Keck headquarters is currently under way.

3. STATUS

The current status is that two segments are out of service due to axial insert cracks, and one segment is out of service due to radial pad cracks. There are four segments in the Keck I telescope, and one in Keck II telescope that we do not want to remove for re-coating until the repair procedures are in place. One segment in Keck II has a failed sensor insert.

The complete failure of an axial insert does not present a danger of major damage to a segment, but a failed insert prevents the whiffletree from distributing the load properly, and the segment cannot be warped. This affects the ability to re-coat segments, due to the lack of spares.

The radial pad cracks are more likely to propagate to such an extent that a large piece of glass could be dislodged which would be difficult or impossible to repair. The state of the radial pads is being carefully monitored until repair procedures are in place. Any segment deemed to be at risk is taken out of service.

Examples from the photo survey of axial insert cracks and how they develop are shown in Figures 7, 8, and 9. The view is looking through the glass from the front surface towards the bottom of the axial insert.

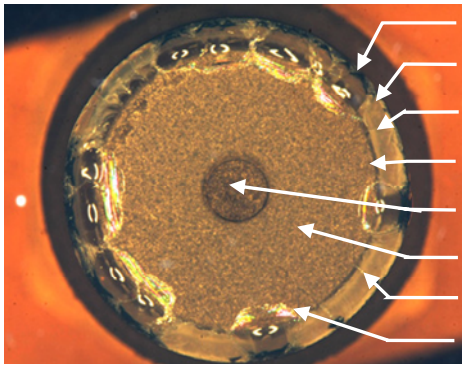

Figure 7

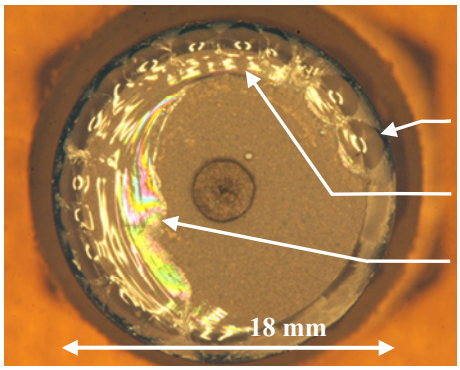

Figure 8

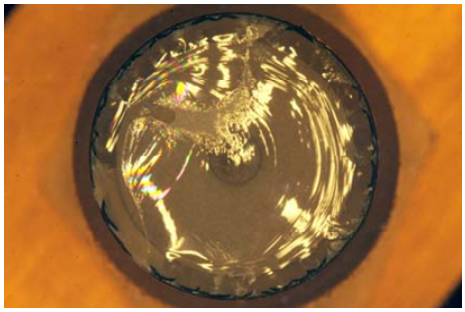

Figure 9

Typical radial pad cracks are shown in Figures 10 and 11.

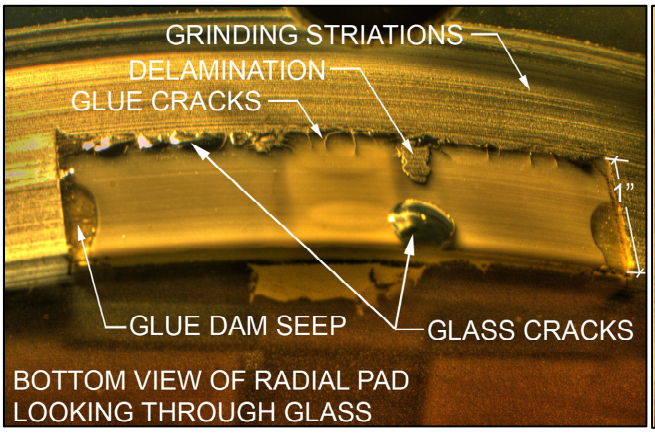

Figure 10

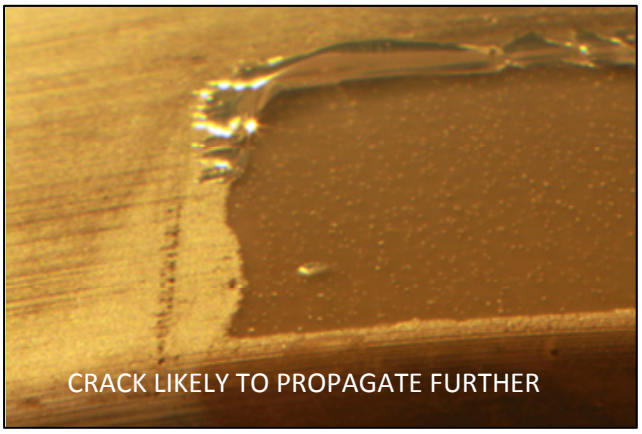

Figure 11

The radial pads were originally installed by holding them in place with an alignment fixture and injecting epoxy beneath the pads. A dam was made around three sides of each pad by using a soft adhesive to secure small Teflon tubes along the edges of the pads. The tubes were removed after the epoxy set.[4] Note in Figure 10 that some of the adhesive for the tubes flowed under the pad.

The low viscosity epoxy adhesive EA-9313 was injected into two slots in the face of the pad until adhesive flowed out of the top edge of the pad. This left a thick fillet of epoxy along the top edge. The fillet generates high stresses in the glass when cooled. Also, epoxy remains in the injection slots. The large round bubble crack seen in Figure 10 is at the bottom of one of the slots. The crack in this location is commonly seen on the radial pads. Many of the radial pad cracks appear to be self-terminating. However, the crack seen in Figure 11extends into the glass and may propagate further.

There are also cracks in the epoxy itself, due to aging. In some locations the epoxy has de-bonded from the glass.

All of the radial pads and axial inserts are photographed through the front surface when the segment has been stripped for re-coating. At this writing, 65 of the total 84 segments have been surveyed.[5] Of these, 71% of the axial inserts have cracks, and 77% have radial pads have cracks. Overall, the severity of the axial insert cracks is substantially greater than for radial pads, and ongoing monitoring indicates that the axial inserts cracks are growing more rapidly than the radial pad cracks.

Classification schemes have been developed for the axial inserts and radial pads to categorize the severity of cracks based on the number, size and location of the cracks. A numerical value from 0 (no cracks) to 5 (failed or near failure) is assigned to each axial insert and radial pad. Summary results are shown in Table 1.

Axial Insert Crack Classification		Crack Class					
		0	1	2	3	4	5
Segments w/ cracks	Qty (%)	0 (0%)	65 (100%)	65 (100%)	56 (86%)	34 (52%)	9 (14%)
Inserts w/ cracks	Qty (%)	939 (29%)	1071 (34%)	598 (19%)	431 (14%)	133 (4%)	13 (0.4%)
Radial Pad Crack Classification		Crack Class					
		0	1	2	3	4	5
Segments w/ cracks	Qty (%)	2 (3%)	63 (97%)	54 (83%)	22 (34%)	2 (3%)	1 (2%)
Pads w/ cracks	Qty (%)	89 (23%)	102 (26%)	150 (38%)	45 (12%)	4 (1%)	1 (0.3%)

Table 1

Statistical analysis was performed to determine if cracks occur systematically. There is no significant difference in the crack distribution based on segment type for axial inserts or radial pads. ($\chi^2 = 4.9$, $\chi^2_{p=.05} = 11.1$).

There is a significant difference in the crack distribution by axial insert location ($\chi^2 = 26.7$, $\chi^2_{p=.05} = 6.0$). Axial inserts supporting the whiffletrees are more likely to have cracks than inserts supporting the sensors. Since the load on the whiffletree inserts is cyclical and greater than the sensor inserts, it is inferred that loading and cyclic fatigue has an influence on the likelihood of cracking. Also, although the humidity on Mauna Kea is generally low, high humidity conditions occur as clouds blow in and during storms. There is evidence of moisture accumulation in the axial insert holes. It is well known that water vapor causes crack growth through the process of stress corrosion cracking.[6]

There is a significant difference in the axial insert crack distribution by telescope fabrication ($\chi^2 = 5.1$, $\chi^2_{p=.05} = 3.8$). An analysis of the number of axial insert cracks versus fabrication date shows the number of cracks in the first 42 mirror segments produced for the Keck I telescope is consistent. However, the number of cracks in segments produced Keck II telescope increased over time. The results for radial pads show a uniform number of pads with cracks by serial number.

4. ROOT CAUSE

Several factors that contribute to the development of cracks have been identified. These are summarized in Figures 12 and 13, and the most significant are discussed below.

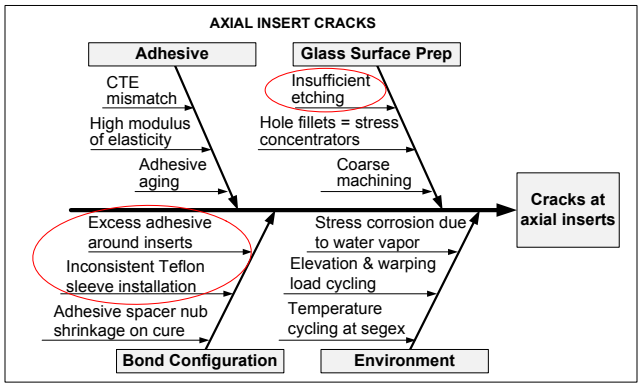

Figure 12

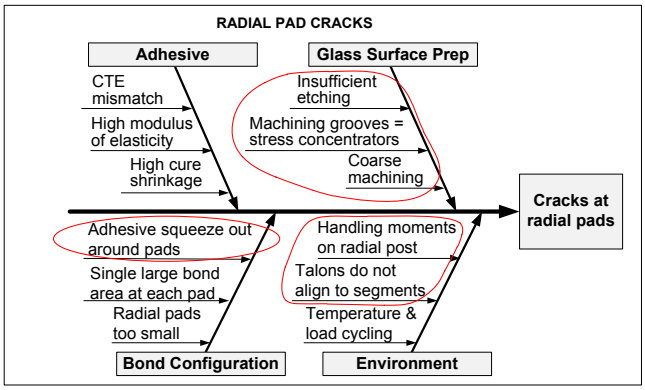

Figure 13

Two key elements for both axial inserts and radial pads are glass surface preparation and the excess unsupported adhesive around the bonds. Subsurface damage (SSD) left from machining is the starting point for crack growth. Schott has shown that the surface strength of Zerodur can be increased greatly by etching sufficiently to remove SSD[7,8]. In general, to produce a high strength surface for bonding, a minimum amount of material must be removed by etching.[9] Mirror segment specifications called for "Acid etching to remove stresses." However, there is no indication how much material was to be removed by etching, or what the final surface profile should be.

For the central radial hole, machining is seen to be very coarse, and there are striations left by the cutting tool. Measurements of a typical surface profile with a Mahr PS1 profilometer, and processed by the NIST Surface Metrology System[10] shows the very rough surface in Figure 14. The mean surface roughness parameter Ra = 8.6 µm. By comparison, Zerodur ground with 240 grit diamond (FEPA D64) typically has a surface roughness parameter Ra less than 2 µm (depending on tool speed and load). Finite element studies have shown that the striations produce stress concentrators that increase stresses by a factor of up to three.

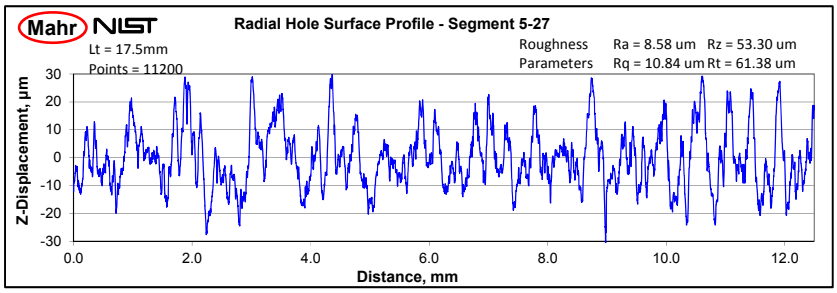

Figure 14

The original axial inserts were bonded at the bottoms of the holes, as in Figure 15. The procedure was to insert a Teflon sleeve into the hole, pour adhesive into the hole, and then push the insert into place. A previously cured nub of adhesive machined to 0.25mm thickness served as a spacer. The Teflon sleeve was removed after the adhesive cured. This method left a layer of unsupported adhesive about 0.5mm to 1 mm thick surrounding the insert which intersects the glass at the fillet, as in Figure 16. The thickness of the adhesive is determined by how far the Teflon sleeve was pushed into the hole. The coefficient of thermal expansion (CTE) of the adhesive is about 83 ppm/ºC.

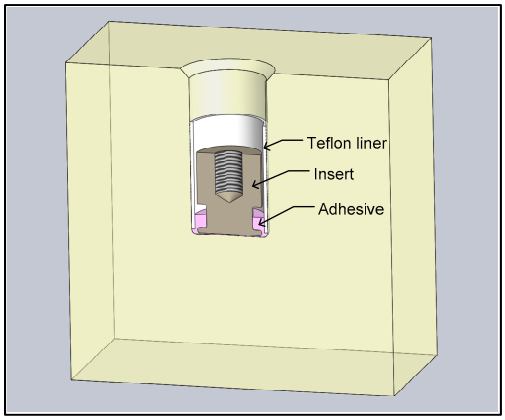

Figure 15

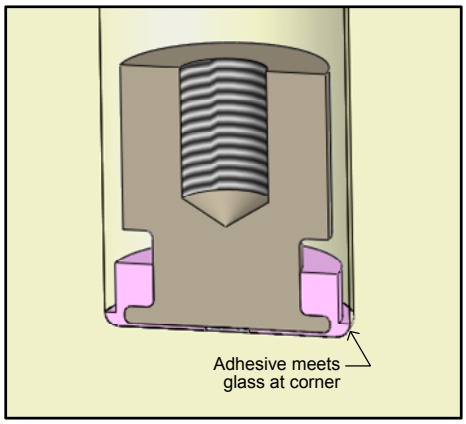

Figure 16

Figure 17 shows a close up of an insert installed into a test block that was made at the time the original segments were fabricated. The thick layer of unsupported adhesive is seen in the right side photo. Notice that the edge of the adhesive meets the glass approximately at the center of the glass fillet, which acts as a stress concentrator.

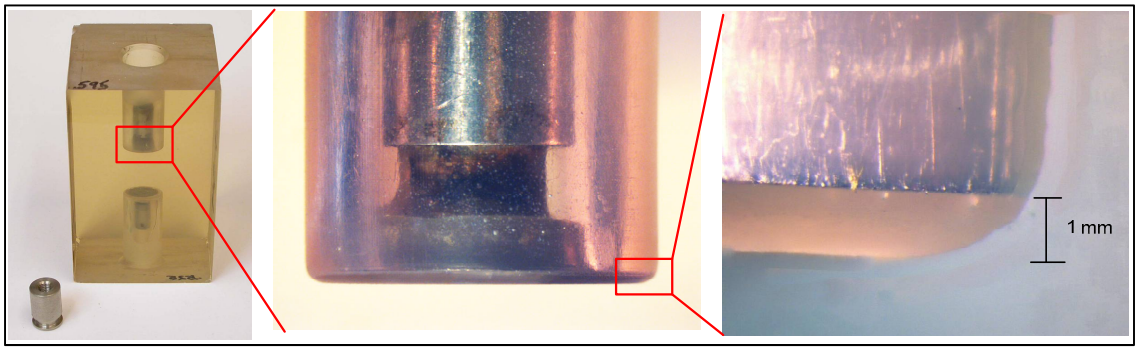

Figure 17

Seen through a polariscope in Figure18, the high stress generated at low temperature is evident.

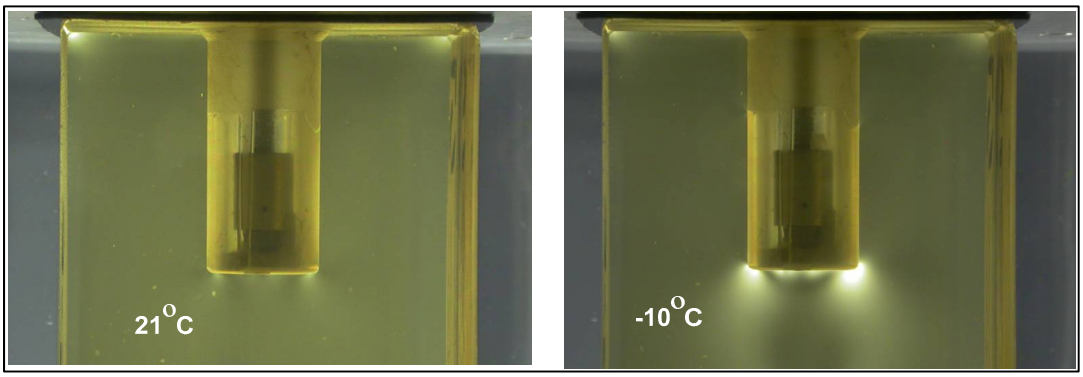

Figure 18

5. MIRROR SEGMENT REPAIR

Evaluation of the extent and growth of axial insert and radial pad cracks led to the conclusion that it is necessary to rebuild all 84 mirror segments with new supports. Due to a number of factors, including space, worker efficiency, and logistics it was decided not to do the repairs at the observatory. A repair facility is currently under construction at the WMKO headquarters in Waimea with workstations for four mirror segments. A protective cradle is being designed to transport the mirror segments safely between the observatory and the repair facility.

The required steps in the repair process have been identified, and detailed procedures are being developed.[11] The original positions of all support hardware (radial post, radial pads, whiffletrees, and axial inserts) will be measured with a high accuracy laser tracker. All of the support hardware and edge sensors will be removed. The original radial pads and axial inserts will be removed and the residual adhesive dissolved by solvents. The glass surface will be machined as necessary to remove cracks, and etched to remove all SSD. New radial and axial supports will be installed. Radial post, whiffletrees, and sensors will be re-installed and re-aligned to the original tolerances with the laser tracker. This process will take about one month per segment. Overall, it is anticipated that repair of all mirror segments can be completed in about four years from the start of production.

Axial Insert Repair

Since the glass at the bottoms of the axial holes is damaged, it is not possible to replace the inserts bonded at the same locations. Several concepts were considered for the repair of axial inserts. These included injecting a filler adhesive into the existing bonds, boring out the holes to bond a new insert at the bottom, and bonding to the back side of the segment. All of these have associated problems that made them unacceptable. The solution that was adopted is to bond new inserts to the circumference of the holes.

A simple method of removing the original axial inserts was developed using a spring loaded tool and induction heater to quickly heat the inserts. This softens the adhesive without locally heating the glass above 70ºC. (Heating Zerodur above 120ºC can affect the CTE of the material.) This same technique has been applied to removal of the radial pads.

The damaged glass at the bottoms of the holes will be ground out. Currently, the options of developing a small portable machine to do this work versus using a large glass capable CNC machine are being considered. The glass will be etched about 100µm in order to insure that all SSD has been removed.

New axial inserts have been designed as shown in Figure 19. These have six "fingers" which are axially stiff but radially compliant. This allows the bond thickness to be maintained at 0.25mm by a shim within the tolerance range of the hole diameter. Also, the fingers can flex radially to adjust for shrinkage of the adhesive on cure and at cold temperature. A tool holds the insert in place while precise amounts of adhesive are injected through small holes in the fingers. There is no adhesive "squeeze out" past the edge of the bonding surfaces. A bonded insert is shown in Figure 20, and a cross-section is in Figure 21.

Figure 19 Figure 20 Figure 21

Radial Pad Repair

Repair of the radial pad cracks presents more difficult challenges than that for the axial inserts. At present, 77% of radial pads have some degree of cracking. Whereas the morphology of cracks in the axial inserts is fairly uniform, radial pads exhibit a variety of cracks, some of which can propagate further into the glass.

Also, the striations in the machined glass surface need to be removed to eliminate stress concentrators. The proposed repair process is to remove the original radial pads, manually grind away the damaged glass, machine the surface to remove the striations, etch the surface to remove SSD, and bond new radial pads clocked 30 degrees from the original positions, as shown in Figure 22.

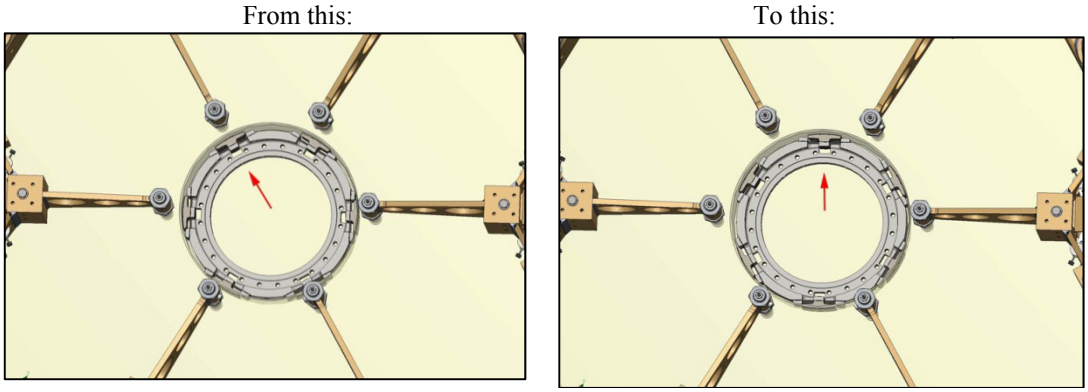

Figure 22

As for the axial inserts, the options of using a small portable tool or CNC for machining are being evaluated. The glass surface will be etched about 100µm to remove all SSD.

A new radial pad and adhesive bonding system are being developed that will provide a larger bonding surface and eliminate the problem of adhesive squeeze out around the pad. Adhesive will be injected through holes in the pads similarly to the new axial inserts.

A segment is removed from the telescope by jacking it up with a tool that attaches to the radial post and pushes it out of the mirror cell. This action applies an axial load on the radial pads, which normally have only in-plane loads. The segment is transferred to a crane that supports the segments around the edges. During the load transfer, and at other points in the handling process, the radial pads are susceptible to excessive overturning loads that can be applied accidentally due to equipment misalignment. Such loads are capable of initiating new cracks in the radial pads, even with the new design. Procedures are in place to reduce the likelihood of such an event. Nevertheless, another project being considered is to redesign the segment removal system so that high loads cannot be placed on the radial pads inadvertently.

6. TESTING AND ANALYSIS

A number of tests have been performed to assess the stresses generated at the mirror segment bonds, and to evaluate the proposed repairs. Some of the significant results are described below.

Finite Element Analysis of radial pad stresses

The conservative nominal bending strength of Zerodur is 10 MPa[12]. The realized bending strength is dependent on the speed of application of stress, and on the surface finish. Bending strength in excess of 100 MPa has been achieved with adequate machining and etching[7].

A large scale finite element analysis (FEA) of the radial pads was performed to evaluate static structural effects of gravity and thermal loading, and dynamic shock effects. The stress produced by overturn loading at the radial pads that would be caused by mishandling during segment exchange was also studied. From the large scale model, sub-models were developed to evaluate the effects of bond line thickness, fillets around the pads due to adhesive squeeze out, and striations in the glass substrate due to machining. Some of the key results of the analysis are:

- The maximum first principal stress at the radial pad bonds due to gravity loading is about 5 MPa. However, stress due to temperature change to the nominal minimum operating temperature of -10ºC can exceed 25 MPa at the edges of the adhesive bonds.
- The stress concentration produced by machining striations under the fillets of unsupported adhesive along the top edge of the radial pads can produce stresses above 50 MPa, depending on the striation depth and period.

- Assuming one edge of a segment is lifted 10mm by the segment handling crane to produce an overturning load on the radial post, the first principal stress at the radial pads exceeds 35 MPa. If the radial post is jammed, the stress can exceed 100 MPa.
- Glass stress at the radial pads increases slightly with decreasing bond line thickness. Bond line thickness variations from 0.6mm to 0.15mm produce an increase in stress of only about 1.5 MPa.

Fracture mechanics analyzes sudden fracture for a single flaw in terms of a stress intensity factor

$$K_I \approx Y\ \sigma_o\ a^{1/2}$$

where Y is a geometry factor, σ_o is the stress normal to the crack plane, and a is the depth of the crack. A crack in a thick plate will result in fracture if

$$K_I \geq K_{IC}$$

where K_{IC} is the critical stress intensity factor for mode I (tensile force normal to the crack plane), and is a material constant determined experimentally.

For mode I fracture K_{IC} = 0.9 MPa $m^{1/2}$ for Zerodur.[13] With Y=2, a normal stress of 10 MPa will produce mode I fracture for an initial crack length of 2mm. With a stress of 50 MPa, fracture will occur for an initial crack length of just 130μm.

Crack growth in Keck mirror segments has been a slow process. Slow (subcritical) crack growth in brittle materials can occur for $K_I << K_{IC}$ due to static loads where moisture is present (stress corrosion cracking), and under cyclic loading (cyclic fatigue). These effects have been studied with finite element fracture mechanics studies. It is clear that the very coarse surfaces of the ground radial and axial holes left subsurface damage that led to the generation of subcritical crack growth, and eventual fracture.

FEA of axial insert stresses

Finite element models of the original and new axial inserts were produced to evaluate the stresses placed on the glass by thermal and mechanical loads[14]. The models show that very high stresses were produced at low temperature by the excess unsupported adhesive in the original installation. The new insert design substantially reduces the glass stress. The conclusions of the FEA studies indicate that for the original axial inserts:

- Where adhesive is applied in between an Invar 36 substrate and Zerodur, the Invar acts to stabilize the adhesive and prevent it from shrinking at low temperature to the extent it would by itself. The unsupported adhesive layer at the bottoms of the axial holes generates very large stress in the glass at low temperature, and the stress generated is approximately proportional to the thickness of the adhesive layer. Thermally induced stress by the unsupported adhesive is much greater than the stress induced by gravity or warping loads.
- The morphology of cracks at axial insert bonds is consistent. However, there is a wide range in the severity of cracks. This varies from insert to insert and from segment to segment. There are a number of variables at production such as ambient temperature, humidity, adhesive mix ratio, handling time, and others which might have some effect. However, the finite element models have identified a single factor which produces substantial variation in thermally induced stress in the unsupported adhesive at the bottoms of the axial holes. As mentioned above, Teflon sleeves were installed into the holes prior to bonding. The thickness of the unsupported adhesive layers at the bottoms of the holes is dependent on how far the Teflon sleeves were pushed into the holes. The thickness of this layer has a substantial effect on the thermally induced stress in the glass. For a 0.5mm layer at -10ºC, the average maximum principal stress at the adhesive edge is 20 MPa. For a 1mm layer, this increases to about 45 MPa. This wide variation serves to explain the difference in crack severity.

For the new inserts analysis was performed to evaluate the effect of bond line thickness, mechanical loading, and adhesive elastic modulus at temperature down to -10ºC. Bond line thickness has minimal effect for bond lines between 0.127mm and 0.381mm. A bond line of .254mm was chosen for use with the new inserts.

The maximum applied load on the axial inserts for both gravity and warping loads is ±310 N. The maximum stress in the glass at the adhesive bonds for both thermal and mechanical loads is less than 10 MPa at -10ºC. For variations in elastic modulus of the adhesive between 1000 MPa to 2500 MPa, the variation in peak stress applied to the glass is roughly proportional to 0.7*(E/E0).

Etching

Etching is a critical step in preparation for bonding to glass to remove SSD. Hydrofluoric acid (HF) is commonly used for etching glass. Due to the risks inherent in handling HF, tests were performed to compare the performance of ammonium bifluoride (NH_4HF_2) as an alternative. Ammonium bifluoride is the active ingredient in chemicals such as ArmourEtch and EtchAll, which are sold in craft stores for frosting glass. Liquid and paste versions are available containing approximately 20% to 30% ammonium bifluoride. Although still releasing fluoride ions, these compounds are less aggressive than HF, and have the perception of being safer to handle.

Glass ceramics such as Zerodur are difficult to etch because of the formation of insoluble fluorides, such as AlF_3, MgF_3, and CaF_2. These form precipitates on the surface during etching which slow the etch rate and result in the formation of uneven surfaces. The addition of hydrochloric acid (HCl) can dissolve the insoluble precipitates and produce a higher quality and more consistent etch.

Schott has recommended an etch solution of HF and HCl in preparation for bonding Zerodur[15]. The mixture used for our tests consists of HF(49%) + HCl(36%) + H_2O in the proportions 2:1:1.5. For ammonium bifluoride, we found that the highest practical concentration at room temperature to avoid super saturation is 50%. Also, the etch rate for ammonium bifluoride slows after about 30 minutes, so multiple etch cycles were performed.

Several test samples were prepared to compare the etch depth and bonding strength of Zerodur etched with HF solution versus ammonium bifluoride solution[16]. The samples were ground to give an initial surface profile Ra = 0.9μm. The etch depth was measured, and block shear tests per ASTM D4501 were performed on 12.7mm diameter coupons bonded with Loctite E-120HP adhesive to evaluate the relative strength of the bonded surfaces. The mean values of test results are shown in Table 2.

Sample Preparation	Etch Depth um	Shear Strength N	Shear stress MPa
Unetched surface	-	1477	11.7
Etch 3 x 30 minutes with NH_4HF_2(50%)	27	2210	17.5
Etch 3 x 30 minutes with [3] NH_4HF_2(50%) + [1]HCl(36%)	35	2349	18.5
Etch 1 x 30 minutes with [2]HF(49%) + [1]HCl(36%) + [1.5]H_2O	86	3149	24.9

Table 2

Etching one time for 30 minutes with HF solution produces a much stronger bond surface than etching three times with ammonium bifluoride solution. Based on these results it was decided that the HF + HCl solution will be used to prepare the Zerodur surfaces for both axial insert and radial pad repairs.

Adhesive selection

Several adhesives were evaluated to use in the mirror segment repairs. Four candidates were selected for testing[17]. These are Armstrong A-12, Hysol Loctite E-120HP, 3M EC-2216 B/A Gray, and Summers Milbond. As a baseline, the original Hysol EA-3913 adhesive was tested. It was decided not to use the EA-9313 adhesive to repair segments for several reasons, including the difficulty of mixing and de-gassing, as well as the low viscosity making it difficult to control the quantity of adhesive applied.

Initial tests have been based on the new axial insert which has been designed. It is anticipated that the same adhesive will be used for radial pad repairs, but tests specific for the radial pads will be conducted. Samples were tested for shear strength, glass stress generated at low temperature, load versus displacement, and creep.

One of the most popular adhesives for structural bonding to glass is 3M EC-2216. It has relatively high strength and low elastic modulus, which minimizes stress induced in glass at low temperature. It has been tested and used extensively by NASA and others. However, it has a low glass transition temperature of 29ºC which makes it questionable for use at room temperature. Mirror segments are at room temperature (~20ºC) during the recoating process. The creep performance tests indicate that it may not be suitable for the mirror segment repairs. Based on the tests, the current candidate adhesive selected for repair of the mirror segments is Loctite E-120HP. Some of the tests that have been performed are described below. Additional testing with larger sample sizes is planned to validate the results.

Strength and adhesion

The new axial inserts will be bonded in shear. Block shear tests were performed to determine the shear strengths of the adhesive bonds. Invar coupons were bonded to etched Zerodur glass blocks and tested to ASTM D4501 standard. Tests were performed with and without adhesive primers. Milbond comes with its own primer, and 3M 3901 silane primer was used for the others. On average, the use of primer increased bond shear strength by about 20%. All of the adhesives proved strong enough to give a strength safety factor of at least 5X.

Stress evaluation

Shrinkage on cure of the adhesive produces some initial stress at glass bonds. At low temperature and with no mechanical loads, the adhesive properties that generate stress are the CTE and elastic modulus. An adhesive may have a high CTE, but if it is soft and stretches easily it does not generate high stresses. In general, the range of CTE values available for adhesives is much smaller than the elastic modulus values. For the adhesives that were studied, the CTE values range from 62 x 10^{-6}/ºC to 102 x 10^{-6}/ºC. However, the elastic modulus values vary from 70 MPa to 2800 MPa. To evaluate the stress generated by the adhesives, a combination of FEA models and tests with a polariscope were performed. As expected, the higher modulus adhesives generated higher stresses in the glass.

Load versus displacement

It is important that the mirror segment supports remain stable and do not allow for motion of the segments with variations in gravity load as telescopes change elevation. Load versus displacement curves were measured for the adhesives at various temperatures. The low elastic modulus adhesives EC-2216 and Milbond exhibited much larger displacements under load than the stiffer adhesives.

Creep

Polymer materials such as adhesives have time dependent viscoelastic properties under load. When a constant load is applied the first response is elastic deformation. If the adhesive were purely elastic, it would reach an equilibrium state for a given load and no additional deformation would occur. However, for viscoelastic materials a sustained load will cause polymer chains to unwind and untangle, allowing them to slide internally. This disentanglement results in additional deformation over time. Once polymer chains have stretched as far as they can, further motion comes from viscous slippage between non-crosslinked chains. This is more prevalent at higher temperatures when the adhesive is near or above its glass transition temperature. Permanent deformation or rupture can occur if the stress, temperature and length of time under load are sufficient. This deformation is termed creep.

Samples of the new axial inserts with the test adhesives were evaluated for creep performance using the standard ASTM D2990 test. Samples were loaded to 150% of the nominal maximum working load at 15ºC. The samples were held at the test load for 24 hours, and the displacement was recorded. At the end of the test, the load was ramped down to no load and the displacement was measured for one hour. The Hysol EA-9313, Armstrong A-12, and Loctite E-120HP adhesives did not show any creep response throughout the test, and there was no indication of permanent plastic deformation. However, the 3M EC-2216 and Milbond adhesives continued to deform throughout the test period and did not return to their initial lengths when unloaded. The permanent plastic deformation of EC-2216 was 20μm and the Milbond deformation was 8μm.

Cyclic loading

Cyclic loading of an adhesive bond can lead to changes in the properties of the adhesive, including changes in elastic modulus and CTE. In order to determine if there are changes in the adhesive properties with large load variations, tests were performed over 5400 cycles at -10ºC on a new axial insert bonded to Zerodur with the candidate adhesive Loctite E-120HP. For this test, the sample was loaded in tension in a sinusoidal pattern with a period of 2 minutes, from 71 N to 468 N, which is 23% to 150% of the maximum in-service load. In this test, dynamic stiffness and energy dissipated per cycle remained constant, indicating that there were no changes in the internal structure of the adhesive.

Evaluation of front surface aberrations

A major concern with replacing the radial pads and axial inserts is that changing the support positions will affect the front surface figure of the mirrors. A full segment finite element model is being constructed to evaluate the effect of changing the support positions. This calculation is expected to give some confidence in the outcome.

To validate the FEA models for the axial inserts, tests were performed on the effects of thermal and mechanical loads in an environmental chamber.[18] Both original and new axial inserts were bonded into 178mm diameter Zerodur flats, and front surface deformations were measured with a Zygo interferometer under varying axial loads and temperatures. The results matched well with the finite element models. The local front surface deformation produced by the original insert at -10ºC is about 20 times greater than that for the new insert. The local deformation due to axial loading on the original insert is about twice the deformation produced by the new insert. This is because the old insert is bonded closer to the front surface, so the load translated to the front is distributed over a smaller area.

Due to the 35 meter focal length of the mirror segments, it is cost prohibitive to perform figure measurements directly with an interferometer or autocollimator. On sky tests with a Shack-Hartmann camera will be used to evaluate the results as segments are rebuilt, using the procedure that is currently applied to warp segments after they are recoated and reinstalled in the telescopes. This test has an accuracy of 15nm rms, which is sufficient to evaluate the optical surface after repair.

Extended life study

One of the questions to be answered is how long will these repairs last. Predicting the lifetime of an adhesive bonded joint is difficult because there are multiple factors such as temperature, moisture and loading that have an effect. Cracks in brittle materials develop over time at lower stress levels than for short term tests.[19] In order to get an estimate of the expected life of the repairs and extended life study will be conducted. The general procedure is to load samples at different percentages of the short term strength (e.g., 80%, 70%, 60%, 50%). The time to failure for each sample is recorded. The data can be extrapolated to estimate the lifetime under actual service conditions. Such tests may be conducted at elevated temperature to accelerate the aging process. An Arrhenius relationship (log failure against reciprocal temperature) is used to calculate the failure rate under normal conditions. Data variance for such tests is high, so a large sample set is needed, and the test may last for more than a year for the lowest stress levels.

7. CONCLUSION

The cracks that have developed at supports in the primary mirror segments over the 20 year life of the Keck telescopes have progressed to the point that repairs are now necessary. Over the last 3 years, extensive surveys and analysis have been performed to evaluate the status of the cracks, determine the underlying causes, and develop a repair strategy. It has been determined that both the axial and radial bonded supports should be replaced.

A new design for the axial inserts has been completed. Preliminary tests indicate that it will perform adequately and will reduce the stress generated in the glass such that new cracks will not form in the future. Additional testing will be performed to insure this result.

A conceptual design for repair of the segment radial pads by clocking the support locations by 30 degrees has been proposed. Finite element models of the mirror segments are being developed to determine if this change will have an effect on the figure of the mirrors. Ultimately, on sky tests will be used to measure the result of the repairs. New handling procedures have been put in place to mitigate the excessive loads that can be placed on the radial pads by misalignment of the lifting systems.

The project is now at the testing and implementation stage. It is anticipated that testing and development of the tools and procedures to perform the repairs will be completed at the end of 2013. The actual repair process is anticipated to take about 4 years.

The exact lifetime of the Keck telescopes is not known. The Mirror Repair Project team is driven by the challenge to insure that the Keck telescopes can continue to perform breakthrough astronomy for many decades in the future.

8. ACKNOWLEDGEMENTS

The W. M. Keck Observatory is operated as a scientific partnership among the California Institute of Technology, the University of California, and the National Aeronautics and Space Administration. The Observatory was made possible by the generous financial support of the W. M. Keck Foundation. The authors wish to recognize and acknowledge the very significant cultural role and reverence that the summit of Mauna Kea has always had within the indigenous Hawaiian community. We are most fortunate to have the opportunity to conduct observations from this mountain.

REFERENCES

1. Schott AG, “TIE-37: Thermal expansion of ZERODUR”, Schott Technical Paper (2006)
2. Nelson, J., “KOTN 163: Optical Parameters of the Keck Telescope”, Keck Observatory Technical Note (1986)
3. Mast, T., Nelson, J., Magner, J, “KOTN 89: Specifications for Generating the Primary Mirror Segments”, Keck Observatory Technical Note (1985)
4. Lawrence Berkeley Laboratory, “Procedures for Segment Assembly at Itek”, Keck Observatory Procedure, TMD-765-Rev G (1989)
5. McBride, D., “KOTN 591: Axial Insert Crack Statistics”, Keck Observatory Technical Note (2011)
6. Wiederhorn, S., Bolz, L., “Stress Corrosion and Static Fatigue of Glass”, J. Am. Ceramic Society, Vol. 53, No. 10 (1970)
7. Hartmann, P., Nattermann, K., Dohring, T., Kuhr, M., Thomas, P., Kling, G., Gath, P., Lucarelli, S., “ZERODUR Glass Ceramics - Strength Data for the Design of Structures with High Mechanical Stresses”, Proc. SPIE Vol. 7018 70180P (2008)
8. Nattermann, K., Hartmann, P., Kling, G., Gath, P., Lucarelli, S., Sesserschmidt, B., “ZERODUR Glass Ceramics – Design of Structures with High Mechanical Stresses”, Proc. SPIE Vo. 7018 70180Q (2008)
9. Hartmann, P., Nattermann, K., Dohring, T., Jedamzik, R., Kuhr, M., Thomas, P., Kling, G., Lucarelli, S., “ZERODUR Glass Ceramics for High Stress Applications”, Proc. SPIE Vol. 7425-22 (2009)
10. National Institute of Standards and Technology, Internet Based Surface Metrology Algorithm Testing System
11. McBride, D., “KOTN 581: Mirror Repair Process Sequence”, Keck Observatory Technical Note (2011)
12. Schott AG, “TIE-33: Design Strength of Optical Glass and ZERODUR”, Schott Technical Paper (2004)
13. Viens, M., “Fracture toughness and crack growth parameters of ZERODUR”, NASA Technical Memo 4185 (1990)
14. McBride, D., “KOTN 587: Finite Element Analysis of Axial Insert Stresses”, Keck Observatory Technical Note (2011)
15. Schott AG, “TIE-45: ZERODUR Adhesive Bonding Recommendation”, (2009)
16. McBride, D., Hudek, J.S., “KOTN 579: Etching Zerodur with Hydrofluoric Acid Vs. Ammonium Bifluoride”, Keck Observatory Technical Note (2011)
17. McBride, D., Hudek, J.S., “KOTN 580: Adhesive Selection for Axial Insert Repairs”, Keck Observatory Technical Note (2011)
18. Panteleev, S., McBride, D., “KOTN 590: Interferometric Tests on 7-Inch Glass Samples”, Keck Observatory Technical Note (2011)
19. Beevers, A., “Durability testing and life prediction of adhesive joints”, International Journal of Materials and Product Technology, Vol. 14, No. 5/6 (1999)